

In Situ Synthesis of Polymer–Clay Nanocomposites from Silicate Gels

Kathleen A. Carrado* and Langqiu Xu

Chemistry Division 200, Argonne National Laboratory, 9700 South Cass Avenue, Argonne, Illinois 60439

Received December 29, 1997. Revised Manuscript Received March 6, 1998

Polymer-containing silicate gels were hydrothermally crystallized to form layered magnesium silicate hectorite clays containing polymers that are incorporated in situ. Gels consist of silica sol, magnesium hydroxide sol, lithium fluoride, and the polymer of choice. Dilute solutions of gel in water are refluxed for various lengths of time and then isolated via centrifugation, washed, and air-dried. Polymer loadings up to 86% were attained by adding more polymer to the solutions after 2-day reaction times, reacting for another 24 h, and continuing this process prior to isolation. Polyaniline (PANI)– and polyacrylonitrile (PACN)–clay samples contain up to 57% and 76% polymer, respectively, after just one sequential addition at high polymer loading. Series of PANI–, PACN–, poly(vinylpyrrolidone) (PVP)–, and hydroxypropylmethylcellulose (HPMC)–clays also were prepared by several sequential additions of lower polymer loading to the silicate gel during crystallization. Final polymer loadings were determined by thermal analysis. Basal spacings between clay interlayers were measured by X-ray powder diffraction for all samples. Increases in polymer loadings and basal spacings were observed for all the neutral polymers studied, until or unless delamination occurred. Delamination was evident for PACN– and PANI–clay nanocomposites. The highest loadings were observed for the PACN–clays, up to 86%. For the cationic polymer polydimethyldiallylammonium chloride, however, the loading could not be increased beyond about 20%. This is due to electrostatic interactions that balance the negatively charged sites on the silicate lattice with those on the cationic polymer chain. Beyond charge compensation, there is no driving force for further incorporation. Charge compensation in the case of the neutral polymers is attained by interlayer lithium(I) cations.

Introduction

The field of polymer nanocomposites strives to enhance polymeric properties by using molecular or nanoscale reinforcements rather than the more conventional particulate-filled microcomposites. Some research has begun to focus on using layered smectite clays as the reinforcing part of the matrix. For example, pioneering work by researchers at Toyota has led to the discovery of nanoscale polymer–clay hybrid composites as promising candidates for lightweight materials applications.¹ There are two end-members which define the realm of structures possible in such nanocomposites.² At one end are the well-ordered and stacked multilayers that result from intercalated polymer chains within host silicate clay layers. At the other end of the spectrum are delaminated materials, in which the host layers have lost all their registry and are well-dispersed in a continuous polymer matrix. This latter case is also referred to as a “house-of-cards” structure to indicate the random and highly disordered nature of the indi-

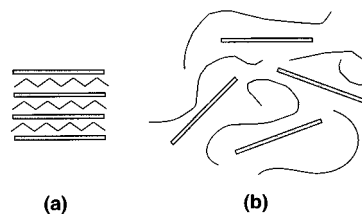


Figure 1. Possible nanoscale polymer-clay hybrid structures formed from natural clays: (a) well-ordered arrays of clay platelets and polymer chains, and (b) well-dispersed clay platelets (delaminated) within a continuous polymer matrix. Both of these cases are shown schematically in Figure 1.

vidual sheets. Both of these cases are shown schematically in Figure 1. Delaminated nanocomposites can attain degrees of stiffness, strength, and barrier properties with far less ceramic content than is used in conventionally filled polymer composites. They are therefore lighter-weight and also exhibit a two-dimensional stability. The higher the degree of delamination in polymer–clay nanocomposites, the greater the enhancement of these properties. The Toyota team has shown that delaminated nylon–clay nanocomposites are improved in strength and modulus compared to both pure nylon and conventional composites, without sacrificing impact resistance.^{1b} The materials also display enhanced heat distortion properties, which extends their use to the engine compartment. Since polymer–clay nanocomposites

* To whom all correspondence should be sent. Telephone: (630) 252-7968. E-mail: kcarrado@anl.gov.

(1) (a) Usuki, A.; Kojima, Y.; Kawasumi, M.; Okada, A.; Fukushima, Y.; Kurauchi, T.; Kamigaito, O. *J. Mater. Res.* **1993**, *8*, 1179. (b) Kojima, Y.; Usuki, A.; Kawasumi, M.; Okada, A.; Fukushima, Y.; Kurauchi, T.; Kamigaito, O. *J. Mater. Res.* **1993**, *8*, 1185. (c) Usuki, A.; Kato, M.; Okada, A.; Kurauchi, T. *J. Appl. Polym. Sci.* **1997**, *63*, 137.

(2) Burnside, S. D.; Giannelis, E. P. *Chem. Mater.* **1995**, *7*, 1597.

achieve composite properties at a lower volume fraction of reinforcement, costly fabrication techniques common to conventional fiber- or mineral-reinforced polymers can be avoided.

The context of the term “clay” is being used here to refer to the class of materials known more specifically as smectite clays. In smectites, individual clay platelets consist of two tetrahedral silicate sheets that are condensed to a central metal oxide octahedral sheet. Aluminosilicates and magnesium silicates are two examples of the compositions that are possible depending upon the type of octahedral metal. Isomorphous substitutions within the lattice, such as Mg(II) for Al(III) or Al(III) for Si(IV), give rise to a net negative charge that is distributed along the entire basal oxygen surface. This charge is compensated for by the presence of exchangeable cations within the interlamellar, or gallery, spaces. The cations are hydrated, and the layers can easily swell to accommodate larger cations or larger amounts of water. The synthetic smectite clay prepared for this work is a magnesium sheet silicate called hectorite.

The synthesis of polymer–clay nanocomposites is currently carried out by one of two methods. Typically, intercalation of a suitable monomer promotes delamination and dispersion of the host layers. This is followed by polymerization of the monomer which yields either linear or cross-linked polymer matrixes. Often, however, the clay must be dispersed using a preliminary preswelling step of long-chain quaternary ammonium intercalation. In situ polymerizations of poly-6-amide (or nylon),^{1a,3} polyethers,⁴ and epoxy^{5,6} have resulted from these methods. Alternatively, direct polymer melt intercalation into a host silicate lattice is done.⁷ These polymers include polystyrene,⁸ poly(ethylene oxide) (PEO),⁹ polypropylene,^{1c,10} and polydimethyl siloxane.² Water-soluble polymers that have formed only intercalated materials via conventional methods include polyethers,¹¹ poly(vinylpyrrolidone) (PVP),¹² and PEO.¹³ In situ polymerization of PVP within a kaolinite clay was successful but did not afford a delaminated product;¹⁴ neither did polyimide^{4,15} or poly(ϵ -caprolactone)¹⁶ in a

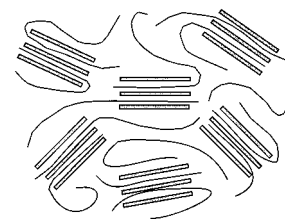


Figure 2. Schematic representation of a synthetic nanoscale polymer–clay hybrid prepared by the direct hydrothermal crystallization method at the 20 wt % final polymer loading level.¹⁹

smectite. In situ polymerization of polyacrylonitrile¹⁷ in a smectite affords incomplete delamination. Here we report a synthetic alternative that is based on the method developed and patented in our laboratories for directly crystallizing silicate clays hydrothermally from a gel containing organics and organometallics,¹⁸ including polymers.¹⁹ There also have been reports of ceramic-reinforced polymers made by hydrolysis of silicate, titanate, or aluminate sol–gels,²⁰ but none to date have involved the crystallization of clay layers.

Results from previous X-ray powder diffraction (XRD) and small angle neutron scattering (SANS) experiments^{19a} have led us to propose a structure for the synthetic polymer–clays, displayed in Figure 2, that can be thought of as a combination of the two shown in Figure 1. Typically, small clay crystallites, intercalated by polymer and stacked to a small degree, are well-dispersed within a continuous polymer matrix. These previously studied materials contain a comparatively small amount of polymer,^{19a} however, at only about 20 wt %. In the current work we have increased the polymer loadings up to as high as 86 wt %, which is more useful for nanocomposite applications. In fact, Toyota’s nylon–clay materials contain only a few wt % clay in the matrix (2–7 wt %); beyond this amount the materials were more difficult to process (casting, extruding, etc.).^{1b} The polymers examined here are poly(vinylpyrrolidone) (PVP), hydroxypropylmethylcellulose (HPMC), polyacrylonitrile (PACN), polydimethylallyl-ammonium (PDDA), and polyaniline (PANI).

Experimental Section

Clay Synthesis. The typical method for in situ hydrothermal crystallization of the polymer–hectorite clays is to create a 2 wt % gel of silica sol, magnesium hydroxide sol, lithium fluoride, and polymer in water and to reflux for 2 days. Complete details can be found elsewhere.²¹ Since the formation of hectorite normally occurs under quite mild conditions, this clay has become our silicate of choice for organic incorporation.²² The organics chosen are usually positively charged to encourage their incorporation into the gallery space via electrostatics. Neutral species including polymers can, how-

(3) Fukushima, Y.; Okada, A.; Kawasumi, M.; Kurauchi, T.; Kamigaito, O. *Clay Miner.* **1988**, *23*, 27.

(4) Pinnavaia, T. J.; Lan, T.; Kaviratna, P. D.; Wang, M. S. *Mater. Res. Soc. Symp. Proc.* **1994**, *346*, 81.

(5) Lan, T.; Kaviratna, P. D.; Pinnavaia, T. J. *Chem. Mater.* **1995**, *7*, 2144.

(6) Messersmith, P. B.; Giannelis, E. P. *Chem. Mater.* **1994**, *6*, 1719.

(7) Vaia, R. A.; Jandt, K. D.; Kramer, E. J.; Giannelis, E. P. *Chem. Mater.* **1996**, *8*, 2628.

(8) Vaia, R. A.; Ishii, H.; Giannelis, E. P. *Chem. Mater.* **1993**, *5*, 1694.

(9) Vaia, R. A.; Vasudevan, S.; Krawiec, W.; Scanlon, L. G.; Giannelis, E. P. *Adv. Mater.* **1995**, *7*, 154.

(10) (a) Kato, M.; Usuki, A.; Okada, A. *J. Appl. Polym. Sci.* **1997**, *66*, 1781. (b) Kawasumi, M.; Hasegawa, N.; Kato, M.; Usuki, A.; Okada, A. *Macromolecules* **1997**, *30*, 6333.

(11) Wu, J.; Lerner, M. M. *Chem. Mater.* **1993**, *5*, 835.

(12) (a) Hild, A.; Sequaris, J.-H.; Narres, H.-D.; Schwuger, M. *Colloids Surf. A* **1997**, *123–124*, 515. (b) Ogawa, M.; Inagaki, M.; Kodama, N.; Kuroda, K.; Kato, C. *J. Phys. Chem.* **1993**, *97*, 3819. (c) Miyata, H.; Sugahara, Y.; Kuroda, K.; Kato, C. *J. Chem. Soc., Faraday Trans. I* **1987**, *83*, 1851.

(13) Aranda, P.; Ruiz-Hitzky, E. *Chem. Mater.* **1992**, *4*, 1395.

(14) Sugahara, Y.; Sugiyama, T.; Hagayama, T.; Kuroda, K.; Kato, C. *J. Ceram. Soc. Jpn.* **1992**, *100*, 413 (CA 117: 10907z).

(15) Lan, T.; Kaviratna, P. D.; Pinnavaia, T. J. *Chem. Mater.* **1994**, *6*, 573.

(16) Messersmith, P. B.; Giannelis, E. P. *Chem. Mater.* **1993**, *5*, 1064.

(17) Bastow, T.; Hardin, S. G.; Turney, T. W. *J. Mater. Sci.* **1991**, *26*, 1443.

(18) Carrado, K. A.; Winans, R. E.; Botto, R. E. U.S. Patent 5,308,808, 1994.

(19) (a) Carrado, K. A.; Thiyagarajan, P.; Elder, D. L. *Clays Clay Miner.* **1996**, *44*, 506. (b) Carrado, K. A.; Thiyagarajan, P.; Elder, D. L. *Synthesis of Porous Materials: Zeolites, Clays, and Nanostructures*; Occelli, M. L., Kessler, H., Eds.; Marcel Dekker: New York, 1997, p 551.

(20) (a) Mark, J. E. *Polym. Engn. Sci.* **1996**, *36*, 2905. (b) Mark, J. E. *Heterog. Chem. Rev.* **1996**, *3*, 307.

(21) Carrado, K. A.; Thiyagarajan, P.; Winans, R. E.; Botto, R. E. *Inorg. Chem.* **1991**, *30*, 794. (b) Carrado, K. A.; Thiyagarajan, P.; Song, K. *Clay Miner.* **1997**, *32*, 29.

ever, also be incorporated.¹⁹ In this scenario excess lithium fluoride is added to the mixture to account for charge compensation. All chemical reagents, including a 30 wt % silica sol DuPont product, were purchased from Aldrich. The polyacrylonitrile (PACN), poly(vinylpyrrolidone) (PVP), and emeraldine salt polyaniline (PANI) were provided with typical average M_w values of 86 000, 10 000, and >15 000, respectively. Polydimethyldiallylammonium chloride (PDDA) was used as a 20 wt % solution in water, with a provided M_w of 100 000–200 000. Hydroxypropylmethylcellulose (HPMC) was obtained from Dow Chemical Co. as Methocel 240S, with a M_w of 1.5×10^6 .

Polymers are added initially at either 20% or 80% by weight loading of the total gel solids components. For example, when 2 g of gel solids (SiO_2 , $\text{Mg}(\text{OH})_2$, LiF) is dispersed in 200 mL, 0.50 g of polymer is added ($0.5/2.5 \times 100 = 20\%$). This mixture is refluxed for 48 h, and then a portion is removed for workup and testing. Another portion of polymer is then added to the remaining slurry, and the mixture is heated for another 24 h. When only one extra addition was made, the second heating was also carried out at 100 °C. When up to four or five repetitions and polymer additions were carried out, the heatings after the first 48-h reflux were performed at only 60 °C. A convention of naming samples as "polymer- n (gel wt %)" is adopted to denote the number of polymer loading sequences (n) at a particular loading (wt %) for each polymer-clay sample. For example, PVP-3 (20%) is synthetic PVP-hectorite after three loadings at 20 wt % polymer as gel solids. This is not to be confused with the wt % polymer determined by DTG in the final nanocomposite samples.

Characterization. XRD analyses were carried out on a Rigaku Miniflex+ instrument using $\text{CuK}\alpha$ radiation, a NaI detector, variable slits, a 0.05° step size, and a 0.50° , $2\theta/\text{min}$ scan rate. Variable slit data could be easily converted to more conventional fixed slit data with the Jade software provided with the instrument, but variable slit data is presented since more information was usually gleaned from these patterns. Powders were loosely packed in horizontally held trays. TGA-DTA (thermal gravimetric analysis and differential thermal analysis) measurements were obtained on an SDT 2960 from TA Instruments. For these samples, measured against an alumina standard in a 100 mL/min O_2 flow with a temperature ramp of $10^\circ\text{C}/\text{min}$ to 800 °C, no major differences were observed between TGA and DTA. The TGA data is also represented in its first-derivative, or differential thermal gravimetry (DTG), format. Total polymer loadings were calculated by measuring the weight loss over the approximate temperature range of 200–600 °C and subtracting the small amount lost over this range for the pure synthetic Li-hectorite (only 2.3 wt %). This results in a conservative estimate of the weight percent organic present in synthetic polymer-hectorites, since the percentage of water loss is expected to be less in these samples. IR measurements were made on a Nicolet 510P FTIR instrument using KBr pellets and a resolution of 2 cm^{-1} .

Results and Discussion

Figure 3 displays representative XRD patterns for the synthetic polymer-clays, in particular PVP- and PACN-hectorites with 28% and 76% final polymer loadings, respectively. A synthetic hectorite with Li(I) exchangeable cations (no polymer) displays a pattern typical of hectorites, with a basal or $d(001)$ spacing of 14.3 Å ($6.18^\circ 2\theta$). This value includes the thickness of the clay layer, which is 9.6 Å for a typical smectite.²³ Peaks at 4.3–4.5 Å (about $20^\circ 2\theta$), 2.56 Å ($35.6^\circ 2\theta$), 1.70 Å ($54^\circ 2\theta$), and 1.51 Å ($61.4^\circ 2\theta$) represent the (110,020), (130,200), (150,240,310), and (060,330) reflec-

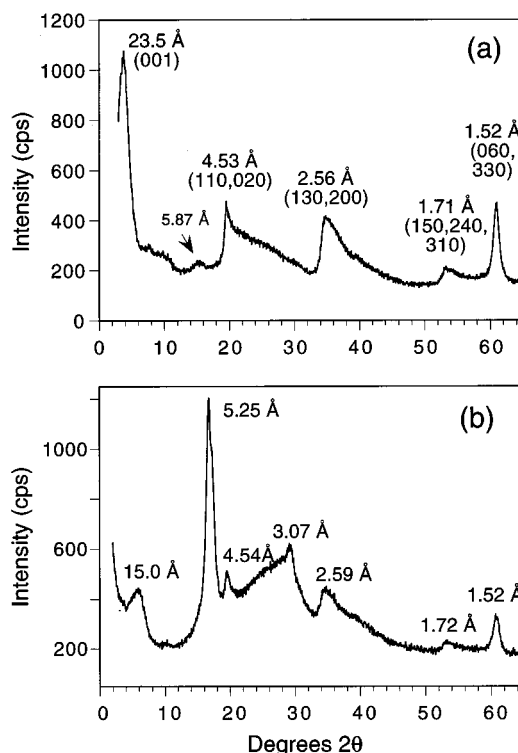


Figure 3. Variable slit XRD patterns of synthetic hectorites prepared with (a) PVP at the 28 wt % final polymer loading level (sample PVP-3 (20%)) and (b) PACN at the 76 wt % final polymer loading level (sample PACN-2 (80%)).

tions of the clay, respectively. There is no sign of unreacted $\text{Mg}(\text{OH})_2$, which would display peaks, among others, at 4.77 Å ($18.6^\circ 2\theta$) and 2.37 Å ($38.0^\circ 2\theta$) for the (001) and (101) reflections of the magnesium hydroxide mineral brucite. The basal spacings increase upon incorporation of polymer, as expected, until or unless delamination occurs. For the PVP-clay sample containing 28% polymer shown in Figure 3a, the $d(001)$ is clearly evident at 23.5 Å and the remainder of the pattern is that of a typical hectorite. The pattern in Figure 3b for PACN-clay with a final polymer loading of 76% is quite different, however. All of the expected clay peaks are present, but the pattern is dominated by new peaks at 5.25 and 3.07 Å. These peaks match the pattern of pure PACN and are visible because of the high concentration of this organic present in the sample. While XRD can indicate delamination by the absence of a $d(001)$, further evidence of delamination is directly observable by transmission electron microscopy;^{1a} these experiments are currently underway.

Figure 4 presents an FTIR spectrum of a synthetic PACN-hectorite (58% polymer loading) as a representative example of organic incorporation by the crystallizing silicate. The clay peaks are manifested by the strong Si-O stretch at 1020 cm^{-1} and the structural -OH stretch at 3679 cm^{-1} . These match very well with previously reported peaks for synthetic hectorite.^{21b} The absence of an -OH stretch at 3699 cm^{-1} for the starting material $\text{Mg}(\text{OH})_2$ confirms the purity of the product. The C-H stretch of the organic occurs at 2940 cm^{-1} , the C-H bend appears at 1454 cm^{-1} , and the C≡N nitrile stretch is clearly evident at 2244 cm^{-1} . The C=O stretch in PVP is observed at 1665 cm^{-1} for synthetic PVP-hectorite samples.

(22) (a) Carrado, K. A.; Forman, J. E.; Botto, R. E.; Winans, R. E. *Chem. Mater.* **1993**, *5*, 472. (b) Carrado, K. A. *Ind. Eng. Chem. Res.* **1992**, *31*, 1654.

(23) Grim, R. E. *Clay Mineralogy*; McGraw-Hill: New York, 1953.

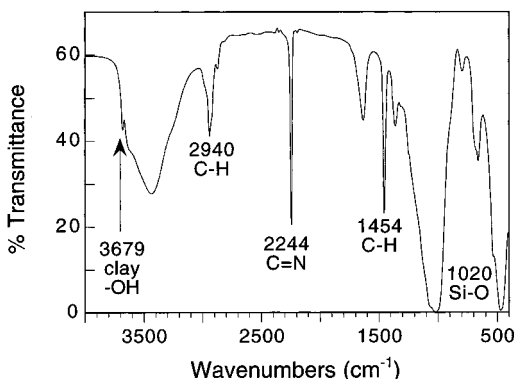


Figure 4. FTIR spectrum of a synthetic hectorite (sample PACN-1 (80%)) containing a final loading of 58% polyacrylonitrile.

Table 1. XRD and DTG Results of Synthetic PVP-, HPMC-, and PDDA-Clays at Sequential Loading Stages

polymer- <i>n</i> ^a (polymer wt % of solids used in gel synthesis)	XRD d(001), Å	total polymer loading (wt %) from DTG ^b
PVP-1 (20%)	18.2	16.8
PVP-2 (20%)	19.8	21.7
PVP-3 (20%)	23.5	27.7
PVP-4 (20%)	24.2	30.4
PVP-5 (20%)	26.0	32.5
PVP-6 (20%)	27.6	34.4
PVP-1 (80%)	22.9	33.1
PVP-2 (80%)	26.0	34.8
HPMC-1 (20%)	16.2	18.1
HPMC-2 (20%)	18.2	26.0
HPMC-3 (20%)	20.8	40.5
HPMC-4 (20%)	23.5	42.3
HPMC-1 (80%)	20.5	41.7
HPMC-2 (80%)	21.8	43.9
PDDA-1 (20%)	15.1	10.2
PDDA-2 (20%)	15.8	16.9
PDDA-3 (20%)	15.4	18.9

^a *n* = loading sequence. ^b The 2.3 wt % loss for Li-hectorite over 200–600 °C has already been subtracted.

Table 2. XRD and DTG Results of Synthetic PACN- and PANI-Clays at Sequential Loading Stages

polymer- <i>n</i> ^a (polymer wt % of solids used in gel synthesis)	XRD d(001), Å	total polymer loading (wt %) from DTG ^b
PACN-1 (20%)	12.6	35.7
PACN-2 (20%)	12.4	63.6
PACN-3 (20%)	12.9	78.1
PACN-4 (20%)	14.6	86.4
PACN-5 (20%)	13.0	70.6
PACN-1 (80%)	12.2	57.3
PACN-2 (80%)	15.0	76.2
PANI-1 (20%)	13.6	20.5
PANI-2 (20%)	13.4	29.1
PANI-3 (20%)	14.2	41.6
PANI-4 (20%)	14.5	43.9
PANI-5 (20%)	14.7	47.6
PANI-1 (80%)	15.9	43.1
PANI-2 (80%)	14.8	57.3

^a *n* = loading sequence. ^b The 2.3 wt % loss for Li-hectorite over 200–600 °C has already been subtracted.

Tables 1 and 2 contain the basal spacings for all of the synthetic polymer–clay samples prepared, along with the percentage of final polymer loading as determined by DTG analysis. Figure 5 displays DTG curves for synthetic Li-hectorite and some of the polymer–hectorites. Surface water loss is represented by the DTG peak at 67 °C, and dehydroxylation of the clay

layers occurs at about 730 °C. Polymer loadings are determined by the percentage of weight lost over the temperature range of about 200–600 °C. The weight percent loadings are increased synthetically by several successive reflux and addition treatments until the effect begins to taper off. For PDPA especially, it is readily apparent that sequential treatments have no effect on increasing the total polymer loading, for it could not be increased beyond 20%. This is due to electrostatic interactions that balance the negatively charged sites on the silicate lattice with those on the cationic polymer chain. Beyond charge compensation, there is no driving force for further incorporation. Charge compensation in the case of the neutral polymers is attained by interlayer lithium(I) cations.

PACN and PANI provide the highest polymer loadings for the synthetic polymer–clays studied. The d(001) values for these nanocomposites, listed in Table 2, are very low at 12–15 Å, and they are also of markedly lower intensity than is normally observed (see Figure 3). These polymers apparently have promoted a large degree of delamination of the hectorite layers. Loss of most of the layer registry will manifest itself in the loss of a basal spacing since the layers are no longer organized in stacks. All of the other (*hkl*) clay peaks are observed, which ensures that clay has indeed been made. As discussed in Introduction, the most desirable polymer–clay nanocomposites comprise the delaminated clay structure.

Using sequential treatments to load the polymer in stages is sometimes the preferred method, because of the concern that initially high polymer solution concentrations may negatively affect the crystallization of the clay layers. This was observed previously when poly(vinyl alcohol) (PVA) was used.^{19a} In this case, the PVA is intercalated between the layers but then the polymer chains apparently cap the edges of the growing silicate layers in some fashion, because only very small particle sizes occur. This, however, did not appear to be the case for any of the polymers studied here. No ill effects to the clay are evident whether several low (20%) loadings are used or just one initially high loading at 80% polymer. In fact, for PVP and HPMC, a maximum of about 34% and 42% polymer is achieved, respectively, in either case. Repeating the 80% loading with another 80% loading resulted in only a 1–2 wt % increase in final polymer uptake. This indicates nearly complete saturation with the first treatment at high polymer concentration with no ill effects to the clay, at least under these conditions.

There are a few previous studies involving the interactions of PVP with clays. In one, the adsorption of PVP with molecular weights ranging from 5000 to 600 000 on the nonswelling clay mineral kaolinite was examined;^{12a} results deal primarily with polymer structure (loops vs flattened coils) in terms of molecular weight and surface coverage. In situ polymerization of PVP within a kaolinite clay has been successful but does not afford a delaminated product.¹⁵ A PVP–tetrasilic mica^{12a} (TSM) has been prepared from an aqueous solution of 1.5:1 PVP:TSM. A basal spacing of 23 Å was reported (gallery about 13 Å) along with a polymer loading of 42%. A molecular thickness for the vinylpyrrolidone monomer of 5.6 Å was calculated, leading to a

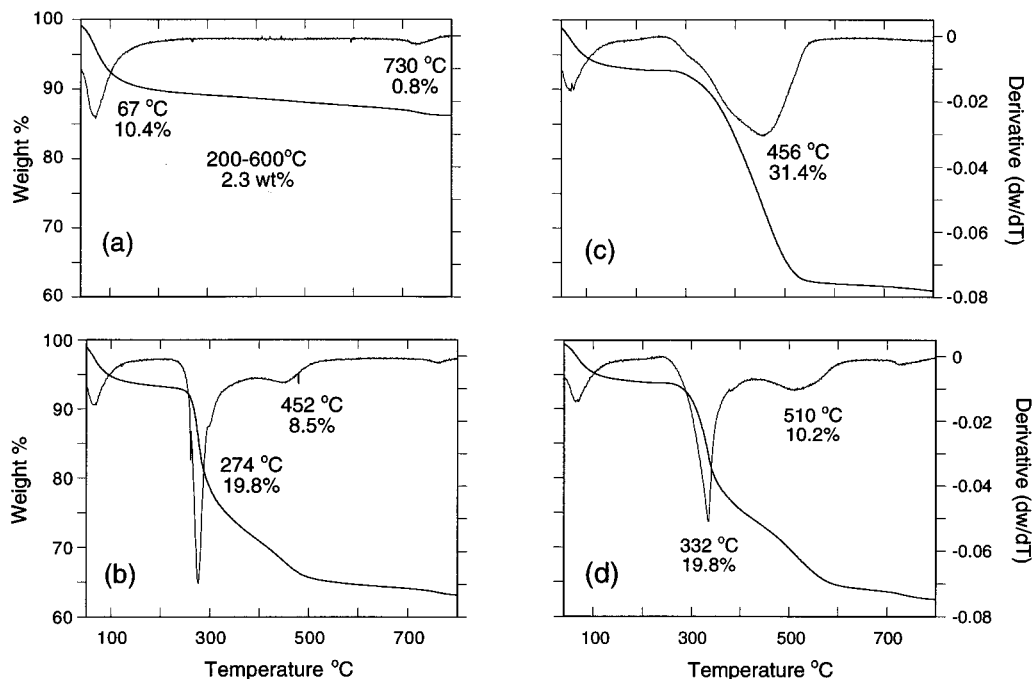


Figure 5. TGA and DTG curves for synthetic hectorite preparations: (a) Li, (b) HPMC-2 (20%), (c) PANI-2 (20%), and (d) PVP-3 (20%). Recall that 2.3 wt % (from 200 to 600 °C in the Li sample) is subtracted from each weight loss before being presented in Tables 1 and 2.

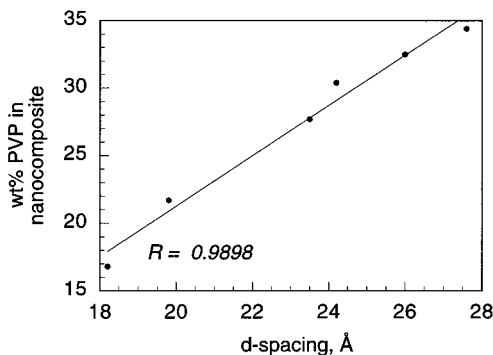


Figure 6. Correlation between d spacing from XRD patterns and weight percent polymer in synthetic PVP-hectorite clay nanocomposites. These samples are from the series made with successive additions of PVP at the 20% loading level (PVP- n (20%), $n = 1-6$; see Table 1).

postulation of bimolecular coverage within the gallery due to bent polymer chains. We are not able to achieve a loading quite this high, and our samples that give a 23 Å basal spacing correspond to only 28% PVP in clay. In fact, Table 1 and Figure 6 display a steady correlation between basal spacing and polymer loading for the synthetic PVP-clays. In another study, a PVP-montmorillonite^{12c} (PVP $M_w = 10\,000$) prepared as above affords a basal spacing of 23.4 Å with 30 wt % PVP, which is similar to our results with hectorite. Hectorite and montmorillonite are in fact very similar clays with respect to structure and layer charge density, differing only in composition (magnesium silicate vs aluminosilicate, respectively). In no case, including ours, has delamination been reported using PVP.

PANI-clays were able to achieve higher loadings at up to 57 wt %. A conventionally made polyaniline-smectite that has been extensively studied by Giannelis²⁴ is of the more structurally ordered type shown in Figure 1a, with a loading of only 20 wt % polymer. Even

at this low loading, the fracture toughness of the hybrid was shown to be superior to that of the clay matrix alone. The in-plane storage modulus for the PANI-clay hybrid was 13 GPa, while for pure silicate and polymer it is only 5.5 and 3 GPa, respectively.²⁴ Bulk polyaniline undergoes a glass transition (T_g) at 220 °C. Above this, the polymer chains undergo motion and behave like a rubber, changing dramatically the stiffness and thermal expansion coefficient. Dynamic modulus and differential scanning calorimetry showed no T_g for their PANI-clay composite, which was attributed to the effect of intercalation and confinement of the polymer chains and the lack of cooperative motion between them.²⁴ It will be interesting to study these properties in the synthetic PANI-clays of higher polymer loadings.

PACN behaves quite differently from all the other polymers examined in our study. First, the final polymer loadings are significantly higher at up to 86 wt %. Second, this maximum value is achieved at an intermediate step within the 20% loading series. Sample PACN-3 (20%) has 78 wt % polymer, PACN-4 (20%) has 86 wt %, and PACN-5 (20%) actually decreases to 71 wt % polymer. This demonstrates at least one case when several low loadings work better than one initially high loading of polymer in the growing silicate gel solution. There is a report that summarizes work on PACN-clays¹⁷ wherein β -sialon is made by heating PACN-montmorillonite to 1300 °C. The PACN-clay precursors are made via in situ polymerization from a montmorillonite preswelled with a long-chain alkylammonium cation, resulting in a sample containing 65 wt % PACN. The XRD pattern is reported as "poorly defined, with a rising baseline in the 30 Å region", and TEM shows a randomly oriented material with small stacks of platelets about 21 Å apart. With either synthetic method, then, PACN has been shown to be

(24) Giannelis, E. P. *J. Miner. Met. Mater. Soc.* **1992**, *44*, 28.

prone to delamination. One last reference of interest concerns a report of a PACN–silica.²⁵ In this organic–inorganic hybrid material the polymer chains are uniformly distributed in and covalently bonded to the silica matrix.

For most naturally occurring smectite clays the aspect ratio of the platelets is fairly large,²⁶ typically in the range of 200–2000. This large aspect ratio may be partly responsible for the enhanced composite properties. However, considering the low loading of the inorganic phase, it has been proposed that the dramatic change in properties is due more to induced ordering of the polymer chains near the polymer–clay interface.²⁴ For a delaminated system, only about 8 wt % clay is sufficient to induce complete ordering of polyimide chains, for example, whereas the amount of silicate required rises to 50% if delamination is not complete (average of 10 layers stacked).²⁴ For laboratory-grown clays, where time is necessarily a factor and can never approach geologic conditions, the aspect ratios are approximately one-third that of natural clays.^{21b} The smaller sheets in fine-grained clays pack in smaller stacks, less regularly. This disorder is inherently similar to the exfoliation or delamination processes that must be forced when using natural clays to make delaminated clay–polymer nanocomposites. This is the advantage to the synthetic alternative presented in this

(25) Wei, Y.; Wang, W.; Yang, D.; Tang, L. *Chem. Mater.* **1994**, *6*, 1737.

(26) Normally, the $<2\ \mu\text{m}$ fraction of natural clays is employed, giving rise to particles in the size range of 2000–20 000 Å. Since one sheet is 10 Å thick, an estimate of the aspect ratio is therefore (2000–20 000)/10, or 200–2000.

work, and it could offer enhanced properties when compared to currently formed clay–polymer hybrids in material testing and processability. These tests are currently underway.

Conclusions

As presented in the Introduction, completely exfoliated and homogeneous dispersions of silicate layers have been achieved in only a relatively small number of cases in the literature, and primarily only when the polymers contain polar functional groups. This has been attributed to the compatibility of the clay's polar hydroxy groups with such polymer functionality.^{10b} Other systems without such polar groups must be intensively modified, such as the case for polypropylene–clay hybrids wherein the clay must be pretreated with stearylammmonium ions and melted with both the polymer and oligomers containing an appreciable number of polar groups.^{10b} This in situ hydrothermal crystallization method has the potential of promoting the high dispersions of silicate layers in a one-step process. Any savings in the number of steps will improve the efficiency of materials preparation. Even more importantly, it is hoped that this process can expand the range of polymers currently under examination, including those that do not contain polar groups.

Acknowledgment. This work was performed under the auspices of the U.S. Department of Energy, Office of Basic Energy Sciences, Division of Chemical Sciences, under Contract No. W-31-109-ENG-38.

CM970814N